Journal of Applied Mechanics and Technical Physics, Vol. 37, No. 3, 1996

NUMERICAL SIMULATION OF SPALLATION IN THICK-WALLED SHELLS UNDER EXPLOSIVE LOADS OF VARIOUS TYPES

A. V. Gerasimov

UDC 539.3

Problems of explosive expansion and failure of thick-walled shells are of interest from the viewpoint of technical applications and attract the attention of specialists [1–4]. The motion of cylindrical shells under the action of detonation products (DP) was discussed by Odintsov et al. [1] in Eulerian formulation and by Levitan et al. [2, 3] in Lagrangian formulation. Relatively uniform strains are typical for expanding shells, while the outflowing detonation products are characterized by very high levels of displacements and strains. Therefore, the Lagrangian approach, which is convenient for study of expansion of closed shells, becomes inapplicable in the case of free DP flow into the surrounding space.

Eulerian description of motion of a continuous medium leads to some difficulties in location and accurate determination of contact and boundary surfaces and in keeping track of fracture zones. These contradictory requirements on the numerical method of calculation of expanding shells can be satisfied by using Euler coordinates to describe DP motion and Lagrange coordinates to describe shell motion. One possible variant of the combined Euler–Lagrange method for solution of problems of expansion of thick elastoplastic shells accompanied by DP effusion into vacuum was proposed by Gerasimov and Lyukshin [4]. This variant is based on a combination of the methods of [5, 6]; it combines the advantages of both methods and avoids their drawbacks. Problems of determination of parameters of the stress-strained state of expanding shells have been extensively investigated, whereas the numerical simulation of shell failure in a three-dimensional axisimmetric formulation has been studied much less [2, 3]. Failure of an elastic shell was studied by Levitan and Moiseenko [2], and failure of an elastoplastic shell caused by a glancing detonation wave was studied by Kostin et al. [3].

Below, using the approach proposed in [4], we study damage growth and the possibility of spallation in the walls of thick-walled elastoplastic shells both under the action of glancing detonation and in throwing of a liner shell onto the internal surface of the main shell. The model of a porous ideal elastoplastic body of [7, 8] is applied to describe the behavior of damaged material. Failure is treated as a process of accumulation and growth of microcracks (micropores) by means of the kinetic equation proposed in [7]. A nonviscous nonthermoconducting gas model was used in description of DP.

1. Statement of the Problem. We study a thick-walled cylindrical elastoplastic shell with the bottom filled with a high-explosive (HE) charge (see Fig. 1a). In the second variant (Fig. 1b) the HE is in contact with a thin liner shell. There is clearance h between the liner and the main shell. On the left end OE the shell is not closed. Initially, a plane detonation wave (DW) is formed at this end. This wave propagates through the HE in the bottom direction. An oblique shock wave proragates along the liner shell, accelerating the particles of the material, while DP effusion into vacuum starts to the left of OE. Note that variants with free effusion of DP from the right end were also considered, i.e., this end was assumed to be open, as was the left end.

The system of equations that describes the motion of a porous elastoplastic medium is based on the laws of conservation of mass, momentum, and energy and has the general form [5, 7, 9]

Institute of Applied Mathematics and Mechanics, Tomsk 634050. Translated from Prikladnaya Mekhanika i Tekhnicheskaya Fizika, Vol. 37, No. 3, pp. 151–159, May–June, 1996. Original article submitted February 20, 1995.

 0021-8944/96/3703-0426 $15.00

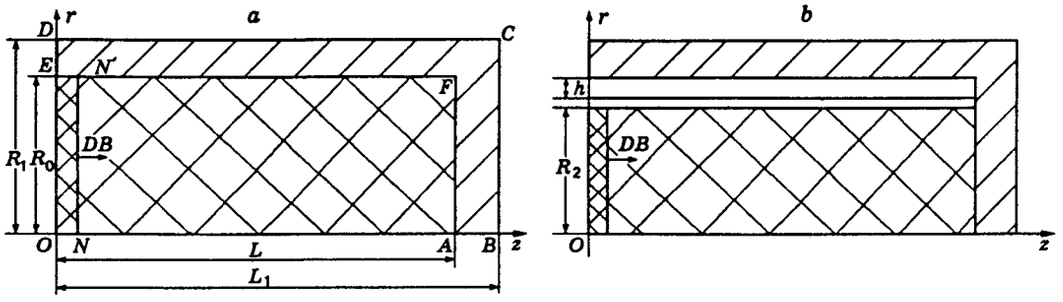

Fig. 1

$$\frac{1}{\rho}\frac{d\rho}{dt}+\frac{\partial v_i}{\partial x_i}=0,\quad \rho\frac{dv_i}{dt}=\frac{\partial S_{ij}}{\partial x_j}-\frac{\partial P}{\partial x_i},\quad \rho\frac{dE}{dt}=S_{ij}\varepsilon_{ij}+\frac{P}{\rho}\frac{d\rho}{dt},\quad S_{ij}=\sigma_{ij}+P\delta_{ij};\tag{1.1}$$

the physical relations were taken in the form of the Prandtl–Reises relation with the Mises flow condition:

$$2\mu\left(e_{ij}-\frac{1}{3}e_{kk}\delta_{ij}\right)=\frac{DS_{ij}}{Dt}+\lambda S_{ij},\qquad S_{ij}S_{ij}=\frac{2}{3}\sigma^2.\tag{1.2}$$

Here x_i are coordinates, t is time, ρ is the current density, v_i are the components of the velocity vector, S_{ij} are the components of the stress deviator, P is the pressure, E is the specific internal energy, ε_{ij} are the components of the strain rate deviator, e_{ij} are components of the strain rate tensor, σ_{ij} are the components of the stress tensor, D/Dt is Yauman's derivative, μ is the shear modulus, σ is the yield point, and δ_{ij} is Kronecker's symbol. The relations are written in Cartesian coordinates for brevity, and transformation to cylindrical coordinates is easily performed. All physical parameters in relations (1.1) and (1.2) refer to a porous medium; they are supplemented by a kinetic equation that describes expansion and compression of spherical pores [7]:

$$\frac{d\alpha}{dt}=\frac{(\alpha_0-1)^{2/3}}{\eta}\alpha(\alpha-1)^{1/3}\Delta P\,\mathrm{sign}\,(P),\quad \alpha=\frac{V+V_s}{V_s},\quad \Delta P=|P|-\frac{a_s}{\alpha}\ln\frac{\alpha}{\alpha-1},$$

where α_0, a_s, and η are material constants, V_s is the specific volume of the continuous component of the porous medium, and V is the specific volume of the pores.

The pressure in the porous medium is determined from the equation of state for the continuous component: $P=P_s(V_s,E)/\alpha$. The equation of state is written in the form [7]

$$P=\frac{K_s(1-(1/2)\Gamma\xi)}{(1-c\xi)^2}+\rho_s\Gamma E.$$

Here the subscript s refers to the matrix material; Γ is the Grüneisen coefficient; c and K_s are material constants; and $\xi=1-\rho_{0s}/\rho_s$. The strength characteristics of the porous material were calculated from the following relations [7, 8]:

$$\sigma=\sigma_s/\alpha,\qquad \mu=\mu_s(1-\Phi)\left(1-\frac{6K_s+12\mu_s}{9K_s+8\mu_s}\Phi\right),\qquad \Phi=(\alpha-1)/\alpha.$$

When the porosity Φ attained the value $\Phi_*=0.3$, the shell material in a given cell was assumed to be damaged.

The system of gas-dynamic equations in Eulerian variables for three-dimensional axisymmetric motion of DP is written as [9]

$$\frac{\partial\rho r}{\partial t}+\frac{\partial\rho ur}{\partial z}+\frac{\partial\rho vr}{\partial r}=0,\qquad \frac{\partial\rho ur}{\partial t}+\frac{\partial(P+\rho u^2)r}{\partial z}+\frac{\partial\rho uvr}{\partial r}=0,$$
$$\frac{\partial\rho v}{\partial t}+\frac{\partial\rho uv}{\partial z}+\frac{\partial(P+\rho v^2)}{\partial r}=-\frac{\rho v^2}{r},\qquad \frac{\partial er}{\partial t}+\frac{\partial(e+P)ur}{\partial z}+\frac{\partial(e+P)vr}{\partial r}=0,\tag{1.3}$$
$$P=P(\rho,E),\qquad e=\rho(E+q^2/2),\qquad q^2=u^2+v^2,$$

where e is the total energy per unit volume of the gas; u and v are the axial and radial components of the velocity vector; ρ is the gas density; E is the internal energy per unit mass of the gas. In the calculations, a DP equation of state in the form of the Landau–Stanyukovich polytrope was used [10].

For the system of equations that describes three-dimensional axisimmetric motion of the shell under the action of DP, the following initial and boundary conditions were specified.

The unperturbed state of the material is used as the initial data for the shell: $\rho = \rho_0$, $\sigma_{ij} = 0$, $v_i = 0$, and $E = 0$. Let us discuss the initial conditions for DP. At $t = 0$, the zone of HE that has detonated degenerates into a line, but some nodes are necessary to begin the calculations [1]. Therefore, in a narrow zone the self-similar distribution of parameters behind the DW front, obtained for the one-dimensional problem of DP effusion from the surface of a plane charge into vacuum, is taken as the initial condition. This distribution for the Landau–Stanyukovich polytrope $P = A\rho^3$ is given in [10]. When an equation of the form of $P = P(\rho, E)$ was used the initial distribution was obtained by numerical solution of the one-dimensional problem of detonation of a plane HE layer using the method of [5].

The boundary conditions are as follows:
at the free surface $BCDE$,

$$\sigma_n = \tau_n = 0,$$

at the symmetry axis AB,

$$v_n = 0, \qquad \tau_n = 0,$$

in the contact zone between the DP and the shell (initial location EN'), $\sigma_n = -P$, $\tau_n = 0$, and $U_n = v_n$. For the DP at the symmetry axis $v = 0$. Until the DW reaches the bottom, it is considered the right boundary of the calculated zone, whose parameters are equal to the parameters at the Chapman–Jouguet point: $\rho = \rho_j$, $P = P_j$, $v = 0$, and $u = u_j$. After the DW reaches on the bottom, conditions similar to the conditions at the inner surface of the shell are specified. Boundary conditions are not specified at the opened left end, because a supersonic regime is realized there and the sonic line passes into the shell [1] as the shell expands. For the shell with a liner (Fig. 1b) the above conditions are supplemented by the contact condition between them: $\sigma_{n1} = \sigma_{n2}$, $v_{n1} = v_{n2}$, and $\tau_{n1} = \tau_{n2} = 0$. Here σ_n and τ_n are the normal and tangential components of the stress vector, v_n and U_n are the components (perpendicular to the contact surface) of the velocity vectors of the shell particles and of the gas particles, respectively, and the subscripts 1 and 2 refer to the liner shell and to the main shell. This condition implies ideal sliding of one shell over the material of the other.

2. Method of Solution. Test Calculations. The problems formulated here were solved using the combined Euler–Lagrange method, which was described in great detail in [4]. Let us dwell briefly on its key features. If the shell motion is considered along a fixed Euler grid, irregular cells appear at the gas–shell interface. To eliminate the inconvenience associated with such cells, the physical region of the gas flow is mapped onto a rectangular calculated zone, i.e., the method of moving Eulerian grids is applied. The system of equations for the shell was solved using a second-order approximation method (of the "cross" type) [5], and the equations for the DP were solved by the MacCormack method [6]. A combined artificial viscosity (the squared viscosity plus the linear one) was used to eliminate nonphysical oscillations behind the shock wave front. The tensor viscosity, which stabilizes the calculation grid against distortions of the "hour glass" type and applies to triangular cells adjacent to the calculated point, was chosen as in [11]. Nonphysical oscillations in the case of a gas were eliminated by monotonization of the solution using the method of [12]. Several test calculations were performed to evaluate the proposed approach.

The experimental (continuous curve) and calculated laws of motion of the outer surface of the shell are compared in Fig. 2. The experimental data are taken from [10]. Here a copper cylindrical shell with inside diameter $D_0 = 2.54$ cm, a length of $12D_0$, and a wall thickness of 0.26 cm was filled with a HE (TG 36/64), in which detonation was initiated at one end by means of a lens, which held the plane DW front within the shell. The law of expansion of a shell outer surface with initial radius of 1.53 cm was determined by a high-speed photorecoder at a distance of $7D_0$ from the point of HE initiation in the direction perpendicular to the shell axis. Experimental data on the velocity of the upper surface of this copper shell thrown by various HE for

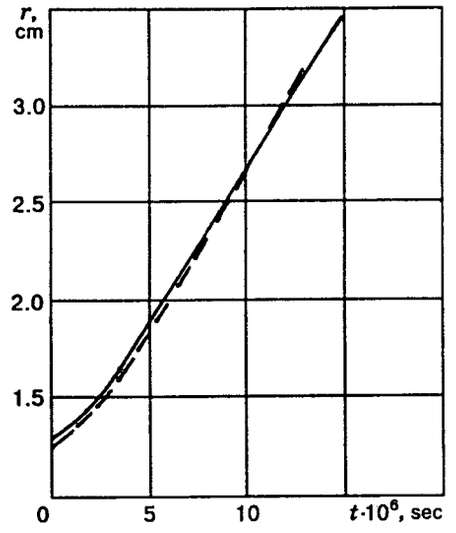

Fig. 2

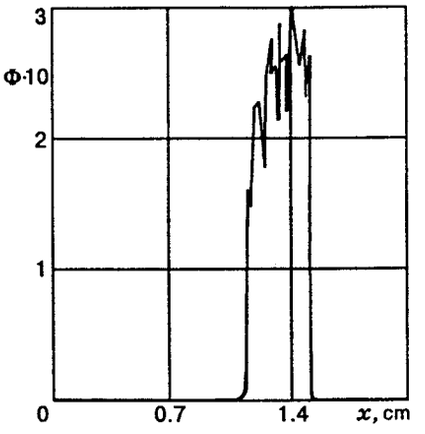

Fig. 3

TABLE 1

HE	ρ_0, g/cm^3	D	u (experiment)	u (calculation)
		km/sec		
Octogen	1.891	9.11	1.68	1.66
TG 36/64	1.717	7.99	1.39	1.41
PETN	1.765	8.16	1.56	1.44
TNT	1.630	6.94	1.18	1.14

detonation initiated at one end of the charge are given in [10]. The velocity of the outer surface of the shell was measured at a distance of 0.5 cm from the initial position.

The calculation results and experimental data for several types of ES are given in Table 1. A comparison of the pressures and velocities during discontinuity decay was performed for glancing detonation and for normal DW incidence on the shell bottom. Analytical solutions of these problems can be found in [10]. A numerical solution was found for copper and hexogen. The calculation results are given in Table 2, where u_c and P_c are the calculated values of the mass velocity and pressure behind the shock-wave front in copper. The error for the glancing DW is relatively higher, because u_c and P_c must be determined in discrete cells of finite length along which the glancing DW front propagates.

The calculation results for the discontinuity decay during the normal collision of the copper inner shell with the steel external shell at a collision velocity of 1500 m/sec, which were obtained by the analytical formulas of [10] and by numerical solution of the problem, give discrepancies of about 3% for pressure and 1% for velocity.

To verify the fracture desintegration model, the one-dimensional problem of collision of two copper plates was solved by the method of [5]. The thickness of the striker plate was one-half that of the target plate. Taking into account the problem's geometry, spallation must occur in the middle of the target plate, and this is confirmed by the obtained result (see Fig. 3). The damage zone is rather narrow and the spall is well-localized.

3. Examples of Computation. Odintsov [13] noted the occurrence of three zones in the cross section of a shell fragment during explosive or impact loading. These are a fragile rupture zone, a zone of internal ruptures or a spalling rupture zone (SRZ), and a shear rupture zone. The SRZ is characterized by numerous

TABLE 2

Detonation type	u_a	u_c	P_a	P_c
	m/sec		GPa	
Glancing	585	550	21.6	22.8
Normal	940	950	45	45.2

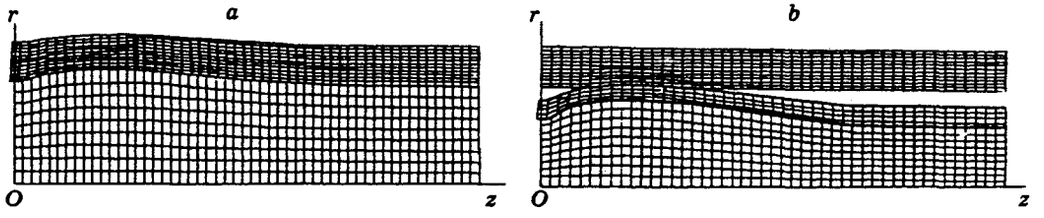

Fig. 4

internal microfractures (pores), which grow and merge to form a main crack on the shell wall. From this zone, fracture can propagate to the inner and outer surfaces of the shell as radial cracks of fragile rupture or shear cracks.

As was noted in [13], the fact that the spallation rupture effects are the first fracture phenomena to occur forces one to consider the dynamic deformation of the shell with allowance for plastic failure of the material and use kinetic equations to describe this failure. The experiments of [14], in which shell expansion was terminated at different stages, and the subsequent metallographic analysis of the cross-sections revealed internal radial cracks that do not emerge on either of the shell surfaces. This confirms the conclusions of [13] on the decisive influence of the SRZ on the formation of main cracks and fragmentation of thick-walled shells. One method of increasing the degree of fragmentation of cylinders is that of using a ringed striking element [13].

Proceeding from the above, in the present work we attempted to simulate numerically the dynamic deformation of thick-walled shells and to study the formation of spallation rupture zones in the walls for various schemes of explosive loading. The calculations were performed for a steel shell without bottom and with the following geometrical parameters: $L = 12$ cm, inside radius $R_0 = 2.4$ cm, and outside radius $R_1 = 3.4$ cm. The physicomechanical properties are as follows: $\rho_0 = 7.86$ g/cm^3, $\mu = 81.4$ GPa, $\sigma = 0.64$ GPa. For the second loading scheme (Fig. 1b), the dimensions of the external shell are the same, for the copper inner liner shell the inside radius is $R_2 = 1.5$ cm, the shell thickness is 0.5 cm, the clearance $h = 0.4$ cm, $\rho_0 = 8.9$ g/cm^3, $\mu = 46$ GPa, and $\sigma = 0.2$ GPa. The explosive substance was desensitized hexogen with initial density $\rho_0 = 1.6$ g/cm^3 and detonation velocity $D = 8{,}000$ m/sec [10].

The strain patterns for the two loading schemes are given in Fig. 4. The current configurations and calculation grids for time moment $t = 10$ μsec are shown. Figure 5 shows damage zones (hatched) in the external shell and zones with critical porosity $\Phi_* = 0.30$ (shaded), for which the material is considered damaged, and the stresses are considered equal to zero during expansion of this calculation cell.

The damage distribution for the first loading scheme is shown in Fig. 5a for time $t = 15$ μsec. The damage is localized near the outer surface, the level of damage is low, and the maximum value of Φ does not exceed 0.02. The damage distribution and spall location for the second loading scheme is shown in Fig. 5b for time $t = 17$ μsec. A zone of continuous increase in porosity Φ of from zero to Φ_* is formed in front of the damaged cells along the generatrix when the detonation wave and the contact point between the outer and inner shells propagate forward. At the left end, the damage level is low, because of the rapid pressure drop in the outflowing gas.

The location of a spallation crack at $t = 6$ μsec during the normal impact of the inner shell on the external shell is shown in Fig. 5c. The external surface of the copper liner had a velocity of 700 m/sec at the

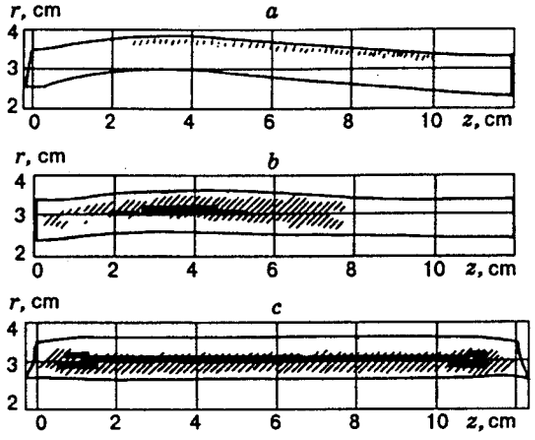

Fig. 5

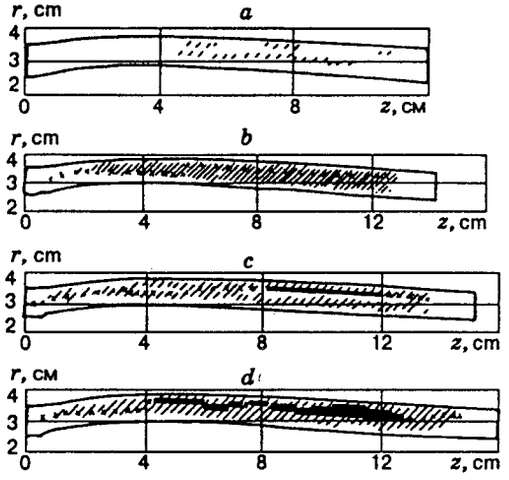

Fig. 6

moment of contact. In the case of the glancing DW, the copper liner moves at about the same velocity. Upon normal collision of the shells, a longer spallation crack formed, compared with that in the second loading scheme. The difference in the damage levels and the occurrence of spallation phenomena are due to the shock-wave amplitude and intensity of the stress fall behind the DW front for the glancing DW and for oblique and normal collisions between the liner and the shell.

The growth in the damage zone and the formation of a spallation crack in the wall of the outer shell as a function of the distance h are shown in Fig. 6. The shell cells in which the porosity reaches a maximum value over the cylinder thickness for the corresponding z coordinate are marked by crosses. To ensure equal duration (16 μsec) of the interaction between the shell and the liner, the shell length and the time of shell expansion were increased in the calculations as h increased. The results shown in Fig. 6a correspond to $h = 0$. In this case the damage level is not high.

The maximum value of porosity Φ is 0.04. An increase in h to 0.1 cm and an increase in time to 20 μsec (see Fig. 6b) lead to growth in the damage zone and to an increase in porosity. In the upper part of the shell the porosity Φ reaches a value of 0.29, which is close to the critical value Φ_*. A spallation crack appears at $h = 0.2$ cm ($t = 22$ μsec), and its further development and expansion are observed at $h = 0.3$ cm ($t = 24$ μsec). These results are given in Figs. 6c and 6d, respectively. The increase in h gives rise to tensile stresses in the shell wall that are sufficient for the growth of damage zones and for the emergence of spallation cracks.

The above results are in agreement with the experimental data of G.yaznov et al. [15], who studied various schemes of explosive loading and shell failures and performed a thorough morphological analysis of the fragments formed. They obtained a moderate damage level for the glancing DW and observed spallation in the shell walls during oblique impact by a liner.

Calculations were performed for an external shell with a thickness of 0.55 cm and $R_0 = 2.4$ cm and for a copper shell with a thickness of 0.2 cm and $R_2 = 1.0$ cm, and the results were compared with the experimental data [16]. The great decrease in the liner thickness during its twofold expansion leads to a sharp increase in computation time according to Courant's requirement. Therefore, the model of a thin incompressible liquid shell [10] was applied to describe the liner, i.e., only the inertial properties of the shell were taken into account. The collision velocity was close to the velocity measured in [16]. The spall layer thickness was 0.165 cm in the experiment and 0.195 cm in the calculations, which can be regarded as good agreement for such an approximate formulation.

The results obtained allow one to draw the conclusion that the loading scheme, its geometry, and the physicomechanical properties of shell material strongly influence the formation of damage zones and the

occurrence of spallation phenomena. The numerical method proposed here allows one to perform qualitative and quantitative evaluations of spall fracture in thick-walled shells and can be applied to create a more general model of cylinder fragmentation under intense dynamical loads.

REFERENCES

1. V. A. Odintsov, V. V. Selivanov, and L. A. Chudov, "Expansion of a thick-walled cylindrical shell under explosive loading," *Izv. Akad. Nauk SSSR, Mekh. Tverd. Tela*, No. 5, 161–168 (1975).
2. Yu. L. Levitan and B. D. Moiseenko, "Numerical simulation of failure of elastic shells under the action of a detonation wave," Preprint No. 5, Inst. Appl. Mat. Acad. of Sci. of the USSR, Moscow (1990).
3. V. V. Kostin, A. S. Reztsov, C. G. Sugak, and V. E. Fortov, "Numerical simulation of explosion-caused failures of thick-walled shells," Preprint No. 25, Inst. of Heat and Mass Transf., Acad. of Sci. of Belorussia, Minsk (1990).
4. A. V. Gerasimov and B. A. Lyukshin, "Numerical solution of the two-dimensional problem of an elastoplastic shell under impulse loading," Deposited at VINITI 03.14.83, No. 1333-83, Moscow (1983).
5. M. L. Wilkins, " Elastoplastic flow calculations," in: *Calculation Methods in Hydrodynamics* [Russian translation], Mir, Moscow (1967).
6. R. W. MacCormack, "The effect of viscosity in hypervelocity impact cratering," AIAA Paper No. 69–354 (1969).
7. J. N. Johnson, "Dynamic fracture and spallation in ductile solids," *J. Appl. Phys.*, **52**, No. 4, 2812–2825 (1981).
8. N. N. Belov, A. I. Korneev, and A. P. Nikolaev, "Numerical analysis of plate failure under impulse load," *Zh. Prikl. Mekh. Tekh. Fiz.*, No. 3, 132–136 (1985).
9. S. K. Godunov (ed.), *Numerical Solution of Multidimensional Gasdynamic Problems* [in Russian], Nauka, Moscow (1976).
10. F. A. Baum, L. P. Orlenko, K. P. Stanyukovich, et al., *Physics of Explosion* [in Russian], Nauka, Moscow (1975).
11. M. L. Wilkins, "Use of artificial viscosity in multidimensional fluid dynamic calculations," *J. Comput. Phys.*, **36**, No. 3, 281–303 (1980).
12. Yu. I. Lobanovskii, "Monotonization of finite-difference solutions in methods of through calculations," *Zh. Vychis. Mat. Mat. Fiz.*, **19**, No. 4, 1063–1069 (1979).
13. V. A. Odintsov, "Mechanics of impulse failure of cylinders," *Tr. MVTU, Problems of Explosion and Impact Physics*, **312**, No. 1, Moscow (1980).
14. E. F. Gryaznov, T. G. Statsenko, S. V. Hahalin, and V. A. Odintsov, "Failure of cylindrical shells at the wave stage," *Tr. MVTU, Mechanics of Impulse Processes*, **399**, Moscow (1983).
15. E. F. Gryaznov, E. V. Karmanov, V. V. Selivanov, and S. V. Hahalin, "Morphology of failure of cylindrical shells at the wave stage," *Probl. Prochn.*, No. 8, 89–92 (1984).
16. E. F. Gryaznov, V. A. Odintsov, and V. V. Selivanov, "Smooth circular spalls," *Izv. Akad. Nauk SSSR, Mekh. Tverd. Tela*, No. 6, 148–153 (1976).